Accepted Manuscript

Design, synthesis, and evaluation of chalcone analogues incorporate α,β-Unsaturated ketone functionality as anti-lung cancer agents via evoking ROS to induce pyroptosis

Min Zhu, Jiabing Wang, Jingwen Xie, Liping Chen, Xiaoyan Wei, Xing Jiang, Miao Bao, Yanyi Qiu, Qian Chen, Wulan Li, Chengxi Jiang, Xiaoou Zhou, Liping Jiang, Peihong Qiu, Jianzhang Wu

PII: S0223-5234(18)30744-X

DOI: 10.1016/j.ejmech.2018.08.072

Reference: EJMECH 10683

To appear in: *European Journal of Medicinal Chemistry*

Received Date: 2 February 2018

Revised Date: 24 August 2018

Accepted Date: 25 August 2018

Please cite this article as: M. Zhu, J. Wang, J. Xie, L. Chen, X. Wei, X. Jiang, M. Bao, Y. Qiu, Q. Chen, W. Li, C. Jiang, X. Zhou, L. Jiang, P. Qiu, J. Wu, Design, synthesis, and evaluation of chalcone analogues incorporate α,β-Unsaturated ketone functionality as anti-lung cancer agents via evoking ROS to induce pyroptosis, *European Journal of Medicinal Chemistry* (2018), doi: 10.1016/j.ejmech.2018.08.072.

Graphical abstract

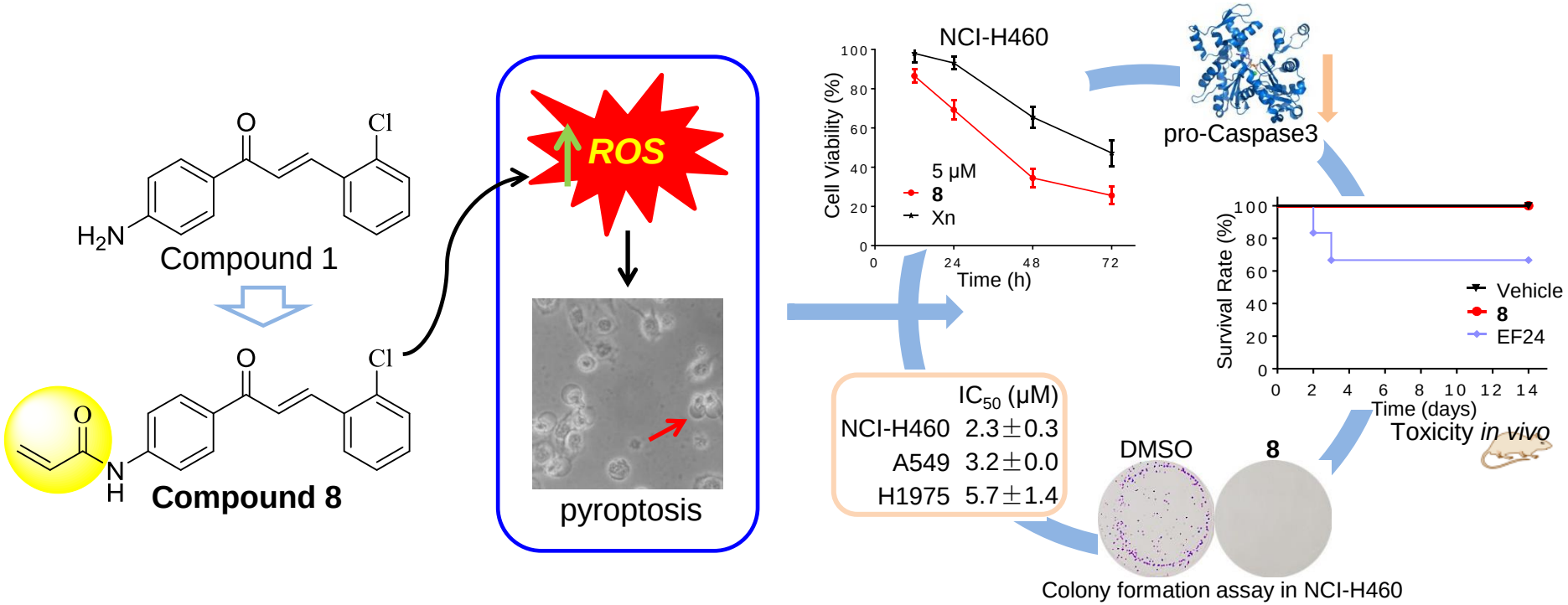

Design, Synthesis, and Evaluation of Chalcone Analogs Incorporate α,β-Unsaturated Ketone Functionality as Anti-lung Cancer Agents via Evoking ROS to Induce Pyroptosis

Min Zhu[a1], Jiabing Wang[ab1], Jingwen Xie[a], Liping Chen[a], Xiaoyan Wei[ca], Xing Jiang[a], Miao Bao[ad], Yanyi Qiu[a], Qian Chen[a], Wulan Li[ae], Chengxi Jiang[a], Xiaoou Zhou[a], Liping Jiang[f], Peihong Qiu[a]*, Jianzhang Wu[a]**

([a]Chemical Biology Research Center, School of Pharmaceutical Sciences, Wenzhou Medical University, Wenzhou, Zhejiang 325035, China)

([b]Municipal Hospital Affiliated to Medical School of Taizhou University, Taizhou, Zhejiang, 318000, China)

([c]Department of Pharmacy, Zhejiang Cancer Hospital, Hangzhou, Zhejiang 310022, China)

([d]Department of Pediatrics, The First Affiliated Hospital of Wenzhou Medical University, Wenzhou, Zhejiang 325035, China)

([e]College of Information Science and Computer Engineering, Wenzhou Medical University, Wenzhou, Zhejiang 325035, China)

([f]Department of Parasitology, Xiangya School of Medicine, Central South University, Changsha, Hunan 410013, China)

([1] These authors contribute to this work equally)

*Correspondence author: Peihong Qiu

Address: Chemical Biology Research Center, School of Pharmaceutical Sciences, Wenzhou Medical University, Wenzhou, Zhejiang 325035, China

E-mail: wjzwzmc@126.com

**Correspondence author: Jianzhang Wu

Address: Chemical Biology Research Center, School of Pharmaceutical Sciences, Wenzhou Medical University, Wenzhou, Zhejiang 325035, China

E-mail: wjzwzmu@163.com

Disclosures/Conflicts of Interest: None declared

Abstract

Chalcone, a natural structure, demonstrates many pharmacological activities including anticancer, and one promising mechanism is to modulate the generation of ROS. It has been known that pyroptosis is associated with anticancer effects, whereas there is fewer researches about ROS-mediated pyroptosis triggered by chemotherapy drugs. Moreover, incorporation of a α,β-unsaturated ketone unit into chalcone may be an effective strategy for development of chemotherapy drugs. Hence, a number of chalcone analogues bearing a α,β-unsaturated ketone were synthesized from chalcone analogues **1** with modest anticancer activities as the lead compound. Structure-activity relationship (SAR) studies confirmed the function of α,β-unsaturated ketone to improve anticancer activity. Notably, compound **8**, bearing a α,β-unsaturated ketone, is the most potent inhibitor of cancer, with IC_{50} values on NCI-H460, A549 and H1975 cells of 2.3±0.3, 3.2±0.0 and 5.7±1.4 μM, respectively. Besides, **8** showed antiproliferative ability against NCI-H460 cells in a time- and concentration-dependent manner through modulating ROS to induce caspase-3-mediated pyroptosis, and displayed a better safety profile *in vivo*. Overall, these results demonstrated that compound **8** is a candidate agent and a potential lead compound for development of chemotherapy drugs, and can be used as a probe to further examine the mechanism of ROS-dependent pyroptosis.

Keywords

Chalcone analogues; α,β-unsaturated ketone; Anticancer effect; ROS; Pyroptosis

1. Introduction

Lung cancer, one of the most leading reasons of morbidity and mortality across the world [1], brings increasing pressure toward human health. Most patients are diagnosed at an advanced stage, which makes them unable to be treated by surgical removal, and chemotherapy is the most primary clinical treatment for them. Currently, there are two main classes of small molecule chemotherapeutic drugs including targeted drugs and cytotoxic drugs [2]. Targeted therapy is widely used because of the strong efficacy for patients with specific genomic aberrations and the fewer side effects. However, mutations frequently happened in lung cancer and thus the successful targeted therapeutic strategy far eluded us [1-3]. What's more, there is not a potentially actionable molecular target for some patients [3], which results in targeted drugs inactive. Hence, it is the first choice to apply the classical cytotoxic drugs for patients ineffective in targeted therapies. However, the cytotoxic agents have more

adverse side effects such as gastrointestinal reaction, liver dysfunction, kidney failure, cardiovascular complications and others [4]. Thus, development of new chemotherapeutic agents with great efficiency and reduced side effects is still very urgent.

At present, the diversity of natural products still provides a critical source of bioactive lead compounds for development of new drugs, which is attributed to their good activity and low toxicity [5-7]. For instance, chalcone, one of the numerous natural compounds, has an extensive distribution in fruits, tea, vegetables and other plants [8-10]. It's also well-known that chalcones demonstrate wide biological activities including anticancer [11], anti-inflammatory [12], analgesic [9], and antioxidant [13], whereas the pharmacological activity ordinarily results in minor effectiveness. It has been reported that the activities of synthetic chalcones were obviously better than natural compounds [14-16]. In our previous study, chalcone derivative **1** was found to possess a modest efficiency on inhibiting proliferation of cancer cells [11], which may be further improved through ulteriorly optimization.

Most recently, Rana et al. has found that the α,β-unsaturated ketone functionality (a Michael acceptor) in the α-methylene-γ-butyrolactone analogues is pivotal for the inhibition of cancer cell growth [17]. And Heller et al. reported that combination of a α,β-unsaturated ketone unit can significantly increase the anticancer activity of triterpenoic acids compounds [18]. These examples showed that incorporating a α,β-unsaturated ketone into a certain molecular structure is able to augment the anticancer properties of secondary natural products [17-22], and α,β-unsaturated ketone can be regarded as functionality structure to drugs design. Therefore, based on remaining the scaffold of compound **1**, we focused on molecular hybridization strategy in order to design and synthesis a series of chalcone analogues bearing α,β-unsaturated ketone scaffold, and evaluated their anti-lung cancer activities, and determined whether α,β-unsaturated ketone group is able to further improve the cytotoxicity.

One of the characterized anticancer mechanisms of chalcones is up-regulating the generation of intracellular reactive oxygen species (ROS) [8, 23-27]. The elevating production of ROS is responsible for the inflammasome-dependent pyroptosis [28-30]. In addition, inflammasomes are found to exhibit anticancer effects through inducing cell pyroptosis [30], a programmed cell death that can also be triggered by chemotherapy drugs in various cancer cell lines [31-33]. Nevertheless, there is no report about the relationship between ROS evoked by chemotherapeutics

and pyroptosis in cancer cells. Thus, in the present study, we started a new anticancer mechanism study of the active compounds and found that increased ROS can result in pyroptosis in lung cancer cells.

2. Results and discussion

2.1 Design and synthesis of chalcone analogues

To increase the anticancer effects produced by a change in the structure of chalcone-based compound **1**, the first series of analogues were obtained by acylation reaction of the amine group on "A" ring of **1**. To our surprise, compared with compound **1**, except compound **8** containing an acrylamide motif, others showed lower cytotoxic against all the tested human lung cancer cell lines, which suggested that α,β-unsaturated carbonyl may strengthen the anticancer activity. Compound **11** was synthesized to investigate the function of α,β-unsaturated ketone located in chalcone skeleton, while retaining the α,β-unsaturated ketone of "A" ring. Furthermore, in order to develop anticancer compounds with higher efficiency, another series of chalcone analogues were designed, and different groups were introduced on "B" ring while "A" ring retained the acrylamide substituents.

The synthesis of two series of chalcone derivatives **2-9** (Table 1) and **12-29** (Table 2) was performed according to the synthetic pathway shown in Scheme 1. Initially, compounds of the first series (**2-9**) were prepared from the lead compound **1** with various acyl chlorides, in the presence of triethylamine as the acid binding agent. Afterwards, another series of chalcone analogues **12-29** were synthesized. 4-aminoacetophenone (**10**) reacted with acrylyl chloride to give the intermediate **11**. Aldol condensation reaction was performed between **11** and a variety of substituted benzaldehyde by using 40% NaOH as the base to give the chalcone derivatives **12-29**. All the chalcone analogues were characterized by LC-MS, HPLC, ^{1}H-NMR and ^{13}C-NMR (Supplementary information). The characteristic data of all products including color, yield, melting points, LC-MS, HPLC, ^{1}H-NMR and ^{13}C-NMR spectrum of compounds were presented in chemistry synthetic section.

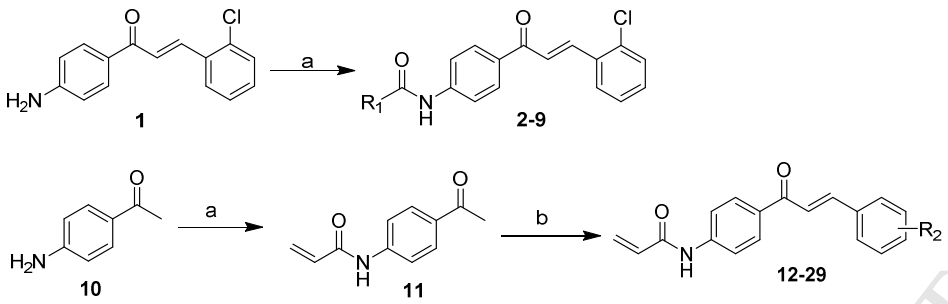

Scheme 1. The general route to produce the chalcone analogues **2-9** and **12-29**. Reagents and conditions: (a): acyl chloride, THF, 0 °C; (b): benzaldehyde, 40%NaOH, EtOH, room temperature.

Table 1. The chalcone analogues **2-9**

Comp.	R_1	Comp.	R_1
2	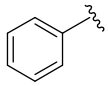	**6**	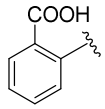
3	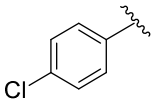	**7**	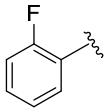
4	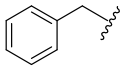	**8**	$-CH=CH_2$
5	$-CH_3$	**9**	$-CH_2CH_3$

Table 2. The chalcone analogues **12-29**

Comp.	R_2	Comp.	R_2
12	2,4-Cl	**21**	2,5-OCH_3
13	4-$N(CH_3)_2$	**22**	2-Br
14	4-OCH_3	**23**	4-Cl
15	2-F	**24**	3,4-Cl
16	2,6-F	**25**	3,4-F
17	3-F	**26**	3,4,5-OCH_3
18	/ [a]	**27**	3,4-OCH_3
19	2,3-OCH_3	**28**	2,3-Cl
20	2-CF_3	**29**	2-F 5-OCH_3

[a] "/" represents none.

2.2 *In vitro* screening of chalcone derivatives against lung cancer cells

The first series of the synthesized chalcone analogues (**2-9**) were evaluated for their *in vitro* antiproliferative activity against three human lung cancer cell lines,

namely, NCI-H460, A549 and H1975, using 3-(4,5-dimethylthiazol-2-yl)-2,5-diphenylte-trazolium bromide (MTT) assay. BMS-345541 (BMS) and Xn (xanthohumol) were used as positive controls. As shown in Figure 1A-C, it is noticeable that most compounds showed lower activity with no clear structural activity relationships (SARs). Among three cancer cell lines, these compounds exhibited relatively larger cytotoxic against NCI-H460 cells. Interestingly, introducing a α,β-unsaturated ketone in compound **8** displayed potent growth inhibition against the three lung cancer cells, which indicated that the Michael acceptor is a favorable feature to increase anticancer potential. Additionally, these results showed that anticancer activity of compound **8** was more pronounced than that of BMS and Xn. Among compounds **1**, **8** and **11**, compared to compounds **1** and **11** with only one α,β-unsaturated ketone, it was found that compound **8** bearing two α,β-unsaturated ketones displayed higher growth inhibition toward cancer cells, which suggested that compound containing two α,β-unsaturated ketones may show more potent anticancer activity.

Based on these results above, in order to obtain more effective anticancer compounds, a series of compound **8** analogues (**12-29**) by varying the substitutions on "B" ring were further developed (Table 2). According to the *in vitro* cytotoxic activities, the structural activity relationships (SARs) of the chalcone analogues **12-29** have been proposed. Close observation of results from Figure 1D-F indicated that almost all compounds selectively displayed higher anticancer activity to the NCI-H460 and H1975 cells, whether electron donating groups or electron withdrawing groups on ring "B". In comparison with compound **18** without substitution on phenyl ring, analogues bearing substitution on phenyl ring showed different levels of anticancer activities, especially compound **13** (4-dimethylamino) and compound **20** (2-trifluoromethyl) showed lower effects on these three cancer cells. Compound **20** with 2-trifluoromethyl substitution on phenyl ring was selectively active on NCI-H460 cells and moderately active on both A549 and H1975 cells. Moreover, results exhibited that analogues **13** (4-dimethylamino), **14** (4-methoxy), **23** (4-chloro), **24** (3,4-dichloro), **25** (3,4-difluoro), and **27** (3,4-dimethoxy) showed potent inhibition on both NCI-H460 and H1975 cells and lower effects on A549 cells. Furthermore, it should be noted that different substitutions on the "B" ring didn't play any significant role in activity to NCI-H460 cancer cells.

Lastly, in recent years, the PAINS (pan-assay interference compounds) present a major problem for medicinal chemistry. PAINS are small molecules that are reactive

under assay conditions and produce false-positive signals [34]. However, several studies have suggested that some PAINS might not be that promiscuous or problematic and could even be true quality probes [35-36]. And it has been emphasized by Gomes et al. that chalcones, as perspective drugs against cancer, bacteria, etc., were mightily underestimated due to the PAINS filtering [10]. In this study, the anticancer efficiencies of these chalcone compounds have been determined by MTT assay, it is possible to exclude that the studied derivatives act in a non-specific way as PAINS. Based on these results, the most active compounds **8**, **22** and **26** from these derivatives were taken-up for further detailed studies.

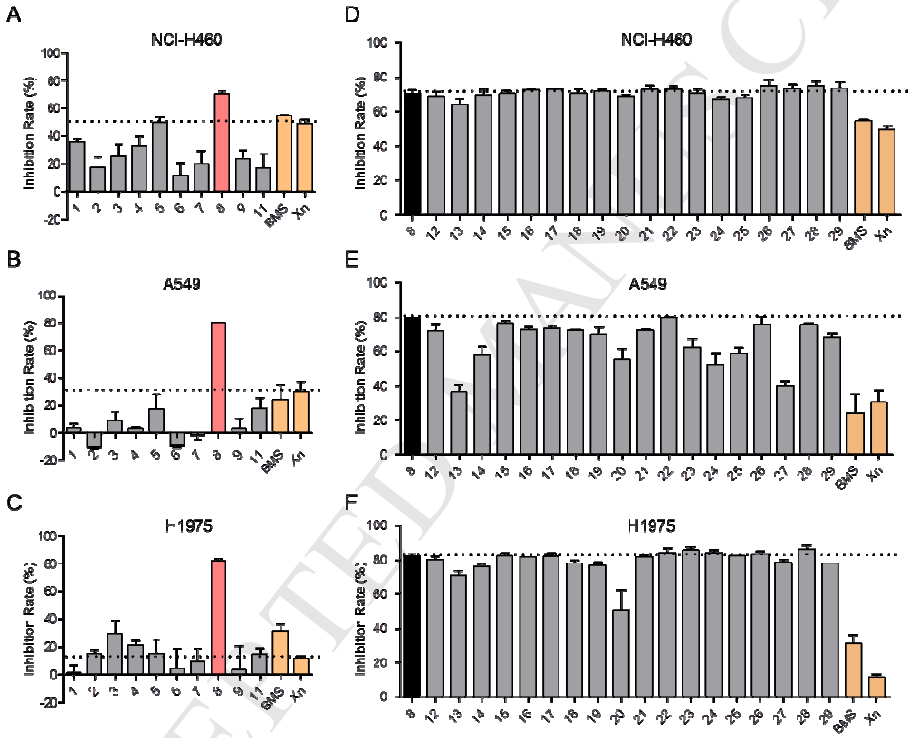

Figure 1. The growth inhibition rate of compounds against NCI-H460 cells (A, D), A549 cells (B, E), and H1975 cells (C, F). The cells were treated with chalcone analogues, BMS and Xn (xanthohumol) at 5 μM for 72 h, finally determined by the MTT assay.

2.3 Active compounds inhibited growth of lung cancer cell lines

On the basis of their promising cytotoxicity, compounds **8**, **22** and **26** were selected for subsequent evaluation of their IC_{50} on three lung cancer cell lines. As listed in Table 3, each compound showed potent growth inhibition on NCI-H460, A549 and H1975 cells with the IC_{50} values in the range of 2.3±0.3-5.7±1.4, 2.2±0.9-5.2±0.7 and 2.0±1.1-5.4±1.2 μM, respectively, which are approximately 2.2- to 3.8-fold more potent than Xn. These results ulteriorly validated that incorporating a α,β-unsaturated ketone unit into chalcone scaffold can significantly enhance their

anticancer effects. Moreover, as shown in Figure 2A, when NCI-H460 cells were treated with compounds **8**, **22** and **26** for a series of times, the population of viable cells decreased in a time-dependent manner. Furthermore, the colony formation assay exhibited that these compounds can obviously restrain the colony formation in a concentration-dependent pattern compared to control group (Figure 2B). More interestingly, all compounds exhibited a greater suppression on colony formation at 2.5 μM than Xn at 5 μM (Figure 2B). Collectively, these data suggested that compounds **8**, **22** and **26** can efficaciously inhibit the growth of three lung cancer cell lines.

Table 3. The IC_{50} (μM) of selected compounds against lung cancer cell lines.

Compound	NCI-H460	A549	H1975
8	2.3±0.3	3.2±0.0	5.7±1.4
22	2.2±0.9	4.4±0.7	5.2±0.7
26	2.0±1.1	4.0±0.5	5.4±1.2
Xn	7.5±2.5	11.9±1.7	13.0±1.3

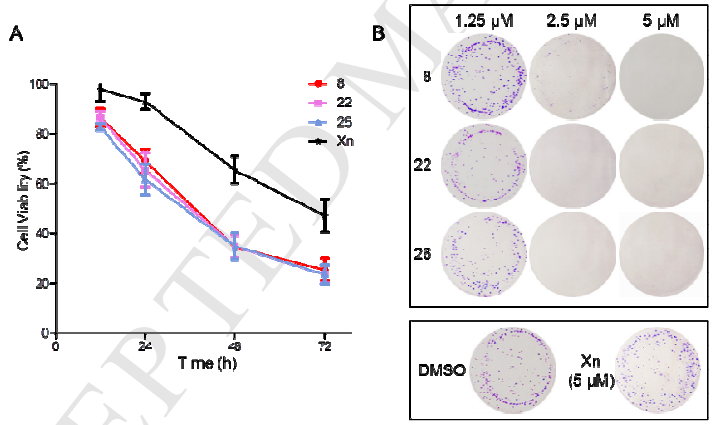

Figure 2. Three active compounds exhibited inhibitory effects on NCI-H460 cells. (A) NCI-H460 cells were treated with compounds **8**, **22** and **26** and Xn at 5 μM for 12, 24, 48 and 72 h, and the cell viability was measured by MTT assay. (B) NCI-H460 cells were exposed to compounds **8**, **22** and **26** at 1.25, 2.5 and 5 μM or Xn at 5 μM. Then medium was changed to fresh medium and allowed to form colonies.

2.4 Compound **8** exhibited anticancer effect by regulating the generation of ROS

ROS are recognized as a pivotal factor in numerous cellular signaling pathways including inflammation, proliferation, metabolism, autophagy, apoptosis, etc [37-39]. The regulation of intracellular ROS levels could be exploited for selective therapeutic approach of cancer, and ROS-based therapeutic strategies continued to be an important direction for research of anticancer agents nowadays. Studies early have

demonstrated that many anticancer agents [40-43] including chalcones are able to up-regulate the production of intracellular ROS. Consequently, based on its better activity, we selected compound **8** in the interest of determining whether the anticancer effect of active compounds are involved in ROS-mediated therapy. Results were showed in Figure 3A, NCI-H460 cells were incubated with 10 μM compound **8** for 3, 6, 12 and 24 h, the levels of intracellular ROS were augmented in comparison to the control group. In addition, the promoted intracellular ROS accumulation induced by **8** was distinctly suppressed by N-acetyl cysteine (NAC), which is one of the ROS scavengers (Figure 3B). Generally, these data suggested that compound **8** can modulate the generation of intracellular ROS.

Afterwards, MTT and colony formation assay were performed to ulteriorly determine if the enhancement of intracellular ROS are responsible for the anticancer activity of compound **8**. As shown in Figure 3C-D, there was almost no cell death after incubation NCI-H460 cells with NAC alone, whereas the growth of cancer cells was significantly suppressed after treating with **8** alone. Moreover, when NAC and compound **8** were applied together, the inhibitory efficacy of compound **8** was evidently attenuated. This indicated that NAC can not only restrain the generation of ROS but also suppress the cell death. Additionally, there was a significant difference between only NAC treated group and compound **8** with NAC treated group, which indicated that NAC can obviously suppress the anticancer effect of **8** (Figure 3C). On the basis of these results, we confirmed that promotion of intracellular ROS levels have a significant function in inducing cell death, and at least partly, explain the anticancer activity of compound **8**.

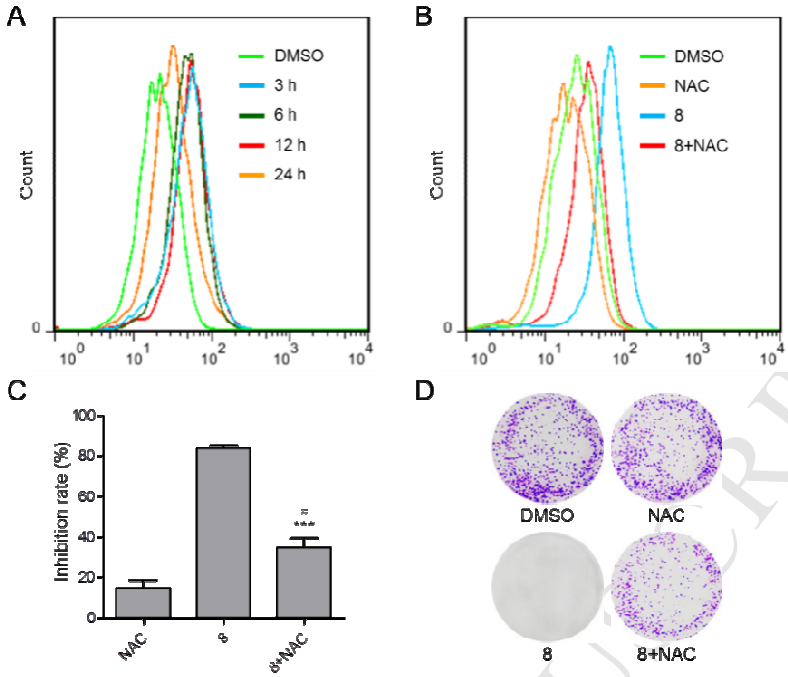

Figure 3. Compound **8** exhibited cytotoxicity against NCI-H460 cells through increasing ROS. (A) ROS levels were measured after treating with **8** at 10 μM for indicated times. (B) Pretreatment with 5 mM NAC for 1 h and then cells were incubated with 10 μM **8** for 3 h. ROS generation were assessed by flow cytometry. (C-D) Cells were pre-incubated with 5 mM NAC for 1 h before exposing to compound **8** (5 μM). (C) Cell viability was measured via MTT assay after treating with **8** for 48 h. *** $P<0.001$ vs only compound **8** treated group. # $P<0.05$ vs NAC treated group. (D) The medium was changed after treating with compound **8** for 12 h and cells were growing in fresh medium for approximately 8 days.

2.5 Compound **8** displayed cytotoxicity against NCI-H460 cells via ROS-based pyroptosis

Pyroptosis is an inflammatory form of lytic programmed cell death. It has been reported that chemotherapy drugs, such as 5-fluorouracil (5-FU) [32] and cisplatin [31], have the ability to trigger pyroptosis in NCI-H460 cells. Therefore, we have sought to investigate whether compound **8** could lead to pyroptosis. As seen in Figure 4A, the morphologic signs of pyroptosis were observed under optical microscope after treatment with **8**, characterized by the loss of osmotic potential, cytoplasmic swelling and cellular content releasing. Likewise, caspase-3 is known to play a key role in NCI-H460 cells pyroptosis triggered by chemotherapy drugs [31]. Then western blot analysis was utilized for studying the expression of this protein. Results showed that compound **8** decreased pro-caspase-3 expression in a time-dependent manner (Figure 4C), which suggested that compound **8** may trigger pyroptosis upon degradation of pro-caspase-3.

What's more, it has been known that the production of ROS is involved in the inflammation-dependent pyroptosis. But there is still fewer researches on the interrelation between pyroptosis and ROS both induced by chemotherapy drugs in cancer cells. Hence, we sought to preliminarily investigate if the increased ROS act on the pyroptosis triggered by compound **8**. NCI-H460 cells were pretreated with NAC for 4 h and then treated with **8**. As shown in Figure 4B, it was found that pyroptosis is suppressed by NAC, and we can draw a conclusion that increased ROS by compound **8** can lead to pyroptosis in lung cancer cells. In summary, these results indicated that compound **8** probably exhibits anticancer efficacy by targeting ROS to trigger caspase-3-mediated pyroptosis in NCI-H460 cells. However, in the previous investigation, V Derange`re [33] discovered that ROS do not affect the occurrence of pyroptosis in human colorectal carcinoma HCT116 cells. Thus it suggested that not all cancer cells' pyroptosis are associated with the increase of ROS. These findings suggested that ROS-dependent pyroptosis may be a new target with promising therapeutic application, and could be explored as an approach for therapy of cancers.

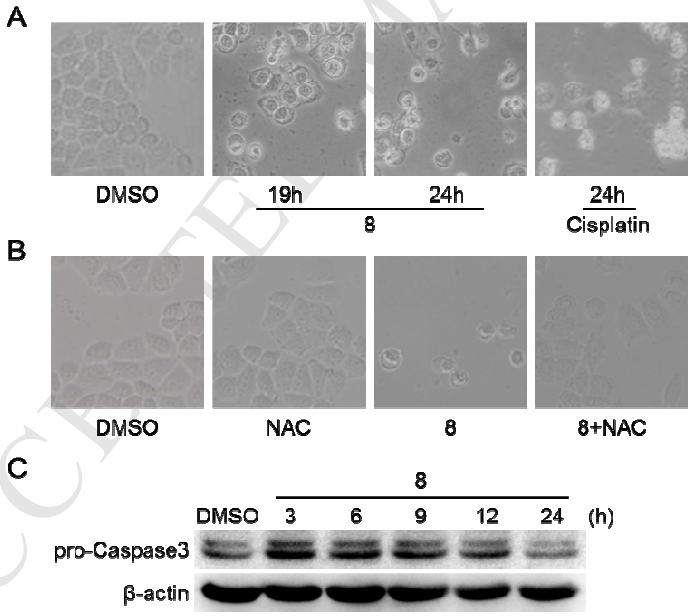

Figure 4. Compound **8** triggered pyroptosis in NCI-H460 cells. (A-B) Static bright field cell images of pyroptosis were obtained with microscopic imaging. (A) Cells were stimulated with 20 μM compound **8** and 20 μg/mL cisplatin for indicated times. (B) NCI-H460 cells were pretreated with NAC (20 mM) for 4 h and then treated with **8** (20 μM) for 24 h. (C) NCI-H460 cells were treated with **8** (5 μM) for indicated times and western blot was performed for detection of pro-caspase-3.

2.6 Toxicity examination of **8** in animal models

In present study, the toxicity exhibited *in vivo* of compound **8** was investigated to aid in future application of active compounds. Therefore, acute toxicity experiment was further carried out to determine the toxicity of compound **8**. Results were showed in Figure 5, no mortality was observed for any of **8**-treated mice while the BALB/c mice treated with EF24, which is a candidate compound with two Michael acceptors [44, 45] and excellent anticancer activities [46, 47], appeared a 33.3% mortality rate. This data suggested that **8** has lower toxicity than EF24. Generally, based on these results, it was confirmed that compound **8** showed a better safety profile in animal models compared with EF24.

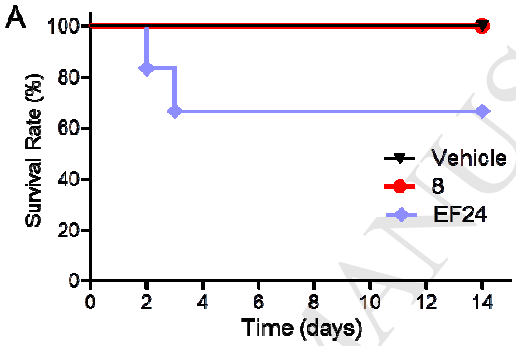

Figure 5. Survival chart of BALB/c mice after treatment with compound **8** in an *in vivo* acute toxicity experiment. All compounds were administrated with a single dose of 500 mg/kg via ip injection at the first day only.

3. Conclusion

In present work, a structural optimization on the lead compound **1** was conducted with the aim to improve the anticancer efficacy. Two series of new chalcone derivatives were designed and synthesized via incorporation of functional groups, and their antiproliferative effects against three lung cancer cells were evaluated. It was found that, in comparison to compound **1**, BMS and Xn, incorporation of a α,β-unsaturated ketone functional group help to markedly increase the antiproliferative efficacy of most compounds. Particularly, compound **8**, bearing a α,β-unsaturated ketone unit, displayed the most potent anticancer effects with the IC_{50} values of 2.3±0.3, 3.2±0.0 and 5.7±1.4 μM, respectively, against NCI-H460, A549 and H1975 cells. Likewise, **8** demonstrated excellent cytotoxicity against NCI-H460 cells in time- and concentration-dependent manner, and was a potent intracellular ROS inducer. Preliminary mechanism studies exhibited that compound **8** significantly induce death of NCI-H460 cells, at least partially, by promoting the levels of intracellular ROS to trigger caspase-3-mediated pyroptosis. More importantly, in

healthy BALB/c mice, ip administration of **8** at 500 mg/kg was found to have a better safety profile than EF24. Taken together, these results indicated that α,β-unsaturated ketone functionality has crucial significance for anti-lung cancer effects of chalcone analogues, and derivative **8** has superior activity *in vitro*, and the mechanism of ROS-mediated pyroptosis deserves further investigating using **8** as a probe.

4. Experimental section

4.1 Chemistry

All chemical reagents and solvents were available from Sigma-Aldrich Aladdin (Beijing, China) and used without further purification. Thin-layer chromatography (TLC) uses silica gel GF25 monitoring reaction, observed by UV light. Mass spectrometry (MS) was performed through an Agilent 1100 LC-MS (Agilent, Palo Alto, CA, USA). Melting point was measured in an opened capillary that under the Fisher-Johns melting apparatus, and uncorrected. Using 600 MHz (^{1}H) and 400 MHz (^{13}C) spectra (Bruker Corporation, Switzerland) record nuclear magnetic resonance spectroscopy (NMR) with TMS as an internal standard. Chemical shifts were performed with $CDCl_3$ and DMSO-*d6*, ^{1}H NMR coupling constants (J) was displayed by hertz (Hz), and multiplicity was expressed as follows: s = singlet, d = doublet, t = triplet, dd = doublet of doublets, m = multiplet. The analysis and purification of HPLC were done an on Agilent 1100 series instrument, using a Agilent ZORBAX SB-C18 column of 4.6 mm i.d.. The purity of all compounds was determined by HPLC analysis to be ⩾95%. Data of novel chemical were pressed as follows:

4.1.1 (E)-N-(4-(3-(2-chlorophenyl)acryloyl)phenyl)benzamide (2)

Pale yellow powder, 50.32% yield, mp 214.1-216.1 °C. ^{1}H-NMR (600 MHz, DMSO-*d6*), δ:10.613 (s, 1H, NH), 8.233 (d, *J*=8.4 Hz, 1H, Ar-H$^{3'}$), 8.224 (d, *J*=8.4 Hz, 2H, Ar-H^{2}, Ar-H^{6}), 8.057 (d, *J*=15.6 Hz, 1H, β-H), 8.021 (d, *J*=15.6 Hz, 1H, α-H), 8.024 (d, *J*=9.0 Hz, 2H, Ar-H$^{2''}$, Ar-H$^{6''}$), 7.991 (d, *J*=8.4 Hz, 2H, Ar-H^{3}, Ar-H^{5}), 7.628 (t, *J*=8.4 Hz, 1H, Ar-H$^{4''}$), 7.580 (d, *J*=9.0 Hz, 2H, Ar-H$^{3''}$, Ar-H$^{5''}$), 7.499-7.462 (m, 2H, Ar-H$^{4'}$, Ar-H$^{5'}$), 7.069 (d, *J*=7.8 Hz, 1H, Ar-H$^{6'}$). ^{13}C-NMR (400 MHz, DMSO), δ: 187.439, 166.014, 143.925, 137.957, 134.556, 134.264, 132.441, 132.334, 131.876, 131.815, 129.983, 129.827×2, 128.544, 128.420×2, 127.782×2, 127.639, 124.853, 119.589×2. HPLC: purity 95.5%. LC-MS m/z: 362.28[M+1]$^{+}$, calcd for $C_{22}H_{16}ClNO_2$: 361.09.

4.1.2 (E)-4-chloro-N-(4-(3-(2-chlorophenyl)acryloyl)phenyl)benzamide (3)

Pale yellow powder, 58.85% yield, mp 182.2-182.5 °C. ^{1}H-NMR (600 MHz,

DMSO-*d6*), δ: 10.668 (s, 1H, NH), 8.010 (d, *J*=9.0 Hz, 2H, Ar-$H^{2''}$, Ar-$H^{6''}$), 7.992 (d, *J*=9.0 Hz, 2H, Ar-$H^{3''}$, Ar-$H^{5''}$), 7.902 (d, *J*=16.2 Hz, 1H, β-H), 7.887 (d, *J*=16.2 Hz, 1H, α-H), 7.581-7.555 (m, 1H, Ar-$H^{6'}$), 7.497-7.439 (m, 2H, Ar-$H^{4'}$, Ar-$H^{5'}$), 7.214 (d, *J*=8.4 Hz, 2H, Ar-H^{2}, Ar-H^{6}), 7.189 (d, *J*=8.4 Hz, 2H, Ar-H^{3}, Ar-H^{5}), 7.031 (d, *J*=8.4 Hz, 1H, Ar-$H^{3'}$). ^{13}C-NMR (400 MHz, DMSO), δ: 187.439, 166.014, 143.925, 137.957, 134.556, 134.264, 132.441, 132.334, 131.876, 131.815, 129.983, 129.827×2, 128.544, 128.420×2, 127.782×2, 127.639, 124.853, 119.589×2. HPLC: purity 96.4%. LC-MS m/z: 396.16$[M+1]^+$, calcd for $C_{22}H_{15}C_{l2}NO_2$: 395.05.

4.1.3 (E)-N-(4-(3-(2-chlorophenyl)acryloyl)phenyl)-2-phenylacetamide (4)

Pale yellow powder, 65.54% yield, mp 171.1-171.9 °C. ^{1}H-NMR (600 MHz, $CDCl_3$), δ: 8.182 (d, *J*=15.6 Hz, 1H, β-H), 8.005 (d, *J*=8.4 Hz, 2H, Ar-H^{2}, Ar-H^{6}), 7.765 (dd, *J*=1.8, 5.4 Hz, 1H, Ar-$H^{3'}$), 7.607 (d, *J*=8.4 Hz, 2H, Ar-H^{3}, Ar-H^{5}), 7.459 (dd, *J*=3.6, 7.2 Hz, 2H, Ar-$H^{5'}$, Ar-$H^{6'}$), 7.435 (s, 1H, α-H), 7.399 (s, 1H, Ar-$H^{4''}$), 7.384 (d, *J*=4.2 Hz, 2H, Ar-$H^{2''}$, Ar-$H^{6''}$), 7.361-7.358 (m, 2H, Ar-$H^{3''}$, Ar-$H^{5''}$), 7.340 (d, *J*=6.0 Hz, 1H, Ar-$H^{4'}$), 3.809 (s, 2H, CH_2). ^{13}C-NMR (400 MHz, DMSO), δ: 187.737, 170.281, 144.337, 138.454, 136.086, 134.717, 132.855, 132.441, 132.257, 130.565×2, 130.422, 129.118, 129.665×2, 128.817, 128.216, 127.115×2, 125.143, 118.962×2, 43.889. HPLC: purity 96.4%. LC-MS m/z: 376.14$[M+1]^+$, calcd for $C_{23}H_{18}ClNO_2$: 375.10.

4.1.4 (E)-N-(4-(3-(2-chlorophenyl)acryloyl)phenyl)acetamide (5)

Pale yellow powder, 50.32% yield, mp 157.6-158.7 °C. ^{1}H-NMR (600 MHz, DMSO-*d6*), δ: 10.340 (s, 1H, NH), 8.202 (d, *J*=8.4 Hz, 1H, Ar-$H^{3'}$), 8.153 (d, *J*=8.4 Hz, 2H, Ar-H^{2}, Ar-H^{6}), 8.019 (d, *J*=8.4 Hz, 1H, β-H), 7.977 (d, *J*=15.6 Hz, 1H, α-H), 7.772 (d, *J*=8.4 Hz, 2H, Ar-H^{3}, Ar-H^{5}), 7.569 (d, *J*=7.8 Hz, 1H, Ar-$H^{6'}$), 7.562-7.075 (m, 2H, Ar-$H^{4'}$, Ar-$H^{5'}$), 2.101 (s, 3H, CH_3). ^{13}C-NMR (400 MHz, DMSO), δ: 187.733, 169.493, 144.451, 138.309, 134.663, 132.282, 132.231, 130.522×2, 129.076, 127.908, 125.284, 118.762×2, 24.659. HPLC: purity 95.6%. LC-MS m/z: 300.04$[M+1]^+$, calcd for $C_{17}H_{14}ClNO_2$: 299.07.

4.1.5 (E)-2-((4-(3-(2-chlorophenyl)acryloyl)phenyl)carbamoyl)benzoic acid (6)

Pale yellow powder, 58.32% yield, mp 165.1-166.5 °C. ^{1}H-NMR (600 MHz, DMSO-*d6*), δ: 8.224 (d, *J*=15.6 Hz, 1H, β-H), 8.170 (d, *J*=9.0 Hz, 2H, Ar-H^{2}, Ar-H^{6}), 7.989 (d, *J*=9.0 Hz, 2H, Ar-$H^{2''}$, Ar-$H^{6''}$), 7.825 (d, *J*=9.0 Hz, 2H, Ar-$H^{3''}$, Ar-$H^{5''}$), 7.770 (dd, *J*=1.8, 7.2 Hz, 1H, Ar-$H^{3'}$), 7.687 (d, *J*=9.0 Hz, 2H, Ar-H^{3}, Ar-H^{5}), 7.514 (d, *J*=15.6 Hz, 1H, α-H), 7.459 (dd, *J*=1.8, 7.2 Hz, 1H, Ar-H^{6}), 7.320-7.368 (m, 2H, Ar-H^{4}, Ar-H^{5}). ^{13}C-NMR (400 MHz, DMSO), δ: 187.330, 168.620, 163.609, 143.543,

143.434, 141.000, 132.812, 132.355, 132.218, 131.532, 129.944×2, 127.762, 126.642, 126.600, 123.325, 118.766×2, 118.475, 117.969, 117.831, 116.971, 116.831. HPLC: purity 97.0%. LC-MS m/z: 404.15 $[M-1]^+$, calcd for $C_{23}H_{16}ClNO_4$: 405.08.

4.1.6 (E)-N-(4-(3-(2-chlorophenyl)acryloyl)phenyl)-2-fluorobenzamide (7)

Pale yellow powder, 50.32% yield, mp 163.6-164.3 °C. ^{1}H-NMR (600 MHz, DMSO-*d6*), δ: 8.200 (d, *J*=15.6 Hz, 1H, β-H), 8.088 (d, *J*=8.4 Hz, 2H, Ar-H^2, Ar-H^6), 7.841 (d, *J*=8.4 Hz, 2H, Ar-H^3, Ar-H^5), 7.769 (d, *J*=7.2 Hz, 1H, Ar-$H^{3'}$), 7.546-7.582 (m, 1H, Ar-$H^{6''}$), 7.516 (d, *J*=15.6 Hz, 1H, α-H), 7.451 (d, *J*=8.4 Hz, 1H, Ar-$H^{6'}$), 7.360-7.315 (m, 4H, Ar-$H^{4'}$, Ar-$H^{5'}$, Ar-$H^{4''}$, Ar-$H^{5''}$), 7.261-7.198 (m, 1H, Ar-$H^{3''}$). ^{13}C-NMR (400 MHz, DMSO), δ: 187.439, 166.014, 143.925, 137.957, 134.556, 134.264, 132.441, 132.334, 131.876, 131.815, 129.983, 129.827×2, 128.544, 128.420×2, 127.782×2, 127.639, 124.853, 119.589×2. HPLC: purity 95.1%. LC-MS m/z: 380.13$[M+1]^+$, calcd for $C_{22}H_{15}ClFNO_2$: 379.08.

4.1.7 (E)-N-(4-(3-(2-chlorophenyl)acryloyl)phenyl)acrylamide (8)

Pale yellow powder, 54.6% yield, mp 176.3-177.3 °C. ^{1}H-NMR (600 MHz, DMSO-*d6*), δ: 10.548 (s, 1H, NH), 8.236 (dd, *J*=1.8, 9.0 Hz, 1H, β-H), 8.204 (d, *J*=9.0 Hz, 2H, Ar-H^2, Ar-H^5), 8.027 (d, *J*=3.6 Hz, 2H, Ar-H^3, Ar-H^6), 7.878 (d, *J*=9.0 Hz, 2H, Ar-$H^{3'}$, α-H), 7.583 (dd, *J*=1.8, 6.0 Hz, 1H, Ar-$H^{6'}$), 7.503-7.464 (m, 2H, Ar-$H^{5'}$, Ar-$H^{4'}$), 6.509-6.464 (m, 1H, CO-CH), 6.333 (dd, *J*=1.8, 15.6 Hz, 1H, CH), 5.841 (dd, *J*=1.2, 8.4 Hz, 1H, CH). ^{13}C-NMR (400 MHz, DMSO), δ: 187.346, 163.757, 163.630, 140.676, 134.107, 133.255, 132.232, 132.005, 131.526, 130.029×2, 128.704, 128.191, 127.814, 125.232, 124.965, 118.809×2. HPLC: purity 96.7%. LC-MS m/z: 312.10$[M+1]^+$, calcd for $C_{18}H_{14}ClNO_2$: 311.07.

4.1.8 (E)-N-(4-(3-(2-chlorophenyl)acryloyl)phenyl)propionamide (9)

Pale yellow powder, 62.78% yield, mp 164.6-167.7 °C. ^{1}H-NMR (600 MHz, $CDCl_3$), δ: 8.135 (d, *J*=15.6 Hz, 1H, β-H), 7.864 (d, *J*=8.4 Hz, 2H, Ar-H^2, Ar-H^6), 7.756 (d, *J*=8.4 Hz, 1H, Ar-$H^{3'}$), 7.582 (d, *J*=8.4 Hz, 2H, Ar-H^3, Ar-H^5), 7.441 (d, *J*=15.6 Hz, 1H, α-H), 7.361-7.333 (m, 2H, Ar-$H^{5'}$, Ar-$H^{6'}$), 7.329-7.308 (m, 1H, Ar-$H^{4'}$), 3.781 (s, 3H, CH_3), 1.216-1.497 (m, 2H,CH_2). ^{13}C-NMR (400 MHz, DMSO), δ: 187.696, 173.141, 144.527, 138.284, 134.735, 132.829, 132.396, 132.143, 130.535×2, 130.487, 129.107, 128.135, 125.130, 118.779×2, 30.179, 9.864. HPLC: purity 99.2%. LC-MS m/z: 314.12$[M+1]^+$, calcd for $C_{18}H_{16}ClNO_2$: 313.09.

4.1.9 N-(4-acetylphenyl)acrylamide (11)

Pale yellow powder, 61.32% yield, mp 142.1-144.9 °C. ^{1}H-NMR (600 MHz, DMSO-*d6*), δ: 10.456 (s, 1H, NH), 7.952 (d, *J*=9.6 Hz, 2H, Ar-H^2, Ar-H^6), 7.841 (d,

J=9.6 Hz, 2H, Ar-H^3, Ar-H^5), 6.497-6.443 (m, 1H, CO-CH), 6.315 (d, *J*=20.4 Hz, 1H, CH), 5.821 (d, *J*=12.0 Hz, 1H, CH), 2.537 (s, 3H, CH_3). ^{13}C-NMR (400 MHz, DMSO), δ: 197.723, 164.274, 142.743, 132.792, 131.038, 129.795×2, 128.935, 119.405, 113.753. HPLC: purity 98.2%. LC-MS m/z: 189.96$[M+1]^+$, calcd for $C_{11}H_{11}NO_2$: 189.08.

4.1.10 (E)-N-(4-(3-(2,4-dichlorophenyl)acryloyl)phenyl)acrylamide (12)

Pale yellow powder, 50.32% yield, mp 214.1-216.1 °C. ^{1}H-NMR (600 MHz, DMSO-*d6*), δ: 10.717 (s, 1H, NH), 8.279 (d, *J*=8.5 Hz, 1H, β-H), 8.200 (d, *J*=8.6 Hz, 2H, Ar-H^2, Ar-H^6), 7.892 (t, *J*=8.4 Hz, 2H, Ar-H^3, Ar-H^5), 7.817-7.772 (m, 2H, Ar-$H^{3'}$, Ar-$H^{6'}$), 7.644-7.564 (m, 2H, Ar-$H^{5'}$, α-H), 6.512 (t, *J*=16.8 Hz, 1H, CO-CH), 6.328 (t, *J*=16.8 Hz, 1H, CH), 5.825 (t, *J*=20.4 Hz, 1H, CH). ^{13}C-NMR (400 MHz, DMSO), δ: 187.564, 164.095, 144.211, 137.143, 135.972, 135.565, 132.547×2, 131.900×2, 130.614, 130.322, 130.005, 128.437, 128.392, 125.780, 119.216×2. HPLC: purity 98.6%. LC-MS m/z: 346.09$[M+1]^+$, calcd for $C_{18}H_{13}Cl_2NO_2$: 345.03.

4.1.11 (E)-N-(4-(3-(4-(dimethylamino)phenyl)acryloyl)phenyl)acrylamide (13)

Pale yellow powder, 53.8% yield, mp 201.4-202.5 °C. ^{1}H-NMR (600 MHz, DMSO-*d6*), δ: 8.048 (d, *J*=8.0 Hz, 2H, Ar-H^2, Ar-H^6), 7.815 (d, *J*=15.0 Hz, 1H, β-H), 7.765 (d, *J*=6.0 Hz, 2H, Ar-H^3, Ar-H^5), 7.565 (d, *J*=6.0 Hz, 2H, Ar-$H^{2'}$, Ar-$H^{6'}$), 7.369 (d, *J*=15.0 Hz, 1H, α-H), 6.710 (d, *J*=8.4 Hz, 2H, Ar-$H^{3'}$, Ar-$H^{5'}$), 6.500 (d, *J*=18.0 Hz, 1H, CO-CH), 6.370-6.325 (m, 1H, CH), 5.827 (d, *J*=12.0 Hz, 1H, CH), 3.063 (s, 6H, NCH_3×2). ^{13}C-NMR (400 MHz, DMSO), δ: 189.230, 163.651, 152.105, 145.677, 141.486, 134.930, 130.983, 130.405×2, 129.684×2, 128.397, 122.769, 119.262, 116.662, 111.882×2, 40.083×2. HPLC: purity 98.6%. LC-MS m/z: 320.87$[M+1]^+$, calcd for $C_{20}H_{20}N_2O_2$: 320.15.

4.1.12 (E)-N-(4-(3-(4-methoxyphenyl)acryloyl)phenyl)acrylamide (14)

Pale yellow powder, 52.5% yield, mp 155.1-157.9 °C. ^{1}H-NMR (600 MHz, $CDCl_3$), δ: 8.051 (d, *J*=8.4 Hz, 2H, Ar-H^2, Ar-H^5), 7.823 (s, 1H, β-H), 7.773 (d, *J*=8.4 Hz, 2H, Ar-H^3, Ar-H^6), 7.623 (d, *J*=8.4 Hz, 2H, Ar-$H^{2'}$, Ar-$H^{6'}$), 7.446 (d, *J*=15.6 Hz, 1H, α-H), 6.960 (d, *J*=8.4 Hz, 2H, Ar-$H^{5'}$, Ar-$H^{4'}$), 6.510 (d, *J*=16.8 Hz, 1H, CO-CH), 6.356-6.311 (m, 1H, CH), 5.845 (d, *J*=10.2 Hz, 1H, CH), 3.879 (s, 3H, CH_3). ^{13}C-NMR (400 MHz, DMSO), δ: 189.076, 163.634, 161.725, 144.505, 141.800, 134.377, 130.894, 130.210×2, 129.839×2, 128.571, 127.706, 119.542, 119.303, 114.460×2, 55.400. HPLC: purity 99.4%. LC-MS m/z: 308.14$[M+1]^+$, calcd for $C_{19}H_{17}NO_3$: 307.12.

4.1.13 (E)-N-(4-(3-(2-fluorophenyl)acryloyl)phenyl)acrylamide (15)

Pale yellow powder, 57.9% yield, mp 177.9-179.2 °C. ^{1}H-NMR (600 MHz, DMSO-*d6*), δ: 10.545 (s, 1H, NH), 8.178 (d, *J*=9.0 Hz, 2H, Ar-H^{2}, Ar-H^{6}), 8.133 (t, *J*=15.0 Hz, 1H, β-H), 8.005 (d, *J*=15.6 Hz, 1H, α-H), 7.878 (d, *J*=9.0 Hz, 2H, Ar-H^{3}, Ar-H^{5}), 7.833 (d, *J*=12.0 Hz, 1H, Ar-H$^{6'}$), 7.526 (d, *J*=7.2 Hz, 1H, Ar-H$^{3'}$), 7.350-7.318 (m, 2H, Ar-H$^{5'}$, Ar-H$^{4'}$), 6.509-6.404 (m, 1H, CO-CH), 6.333 (d, *J*=15.6 Hz, 1H, CH), 5.838 (d, *J*=11.4 Hz, 1H, CH). ^{13}C-NMR (400 MHz, DMSO), δ: 188.994, 163.686, 162.775, 160.749, 142.146, 137.278, 131.806, 131.736, 130.863, 130.031×2, 129.761, 128.642, 124.478, 124.413, 119.350, 116.371, 116.196. HPLC: purity 99.5%. LC-MS m/z: 296.10[M+1]$^{+}$, calcd for $C_{18}H_{14}FNO_2$: 295.10.

4.1.14 (E)-N-(4-(3-(2,6-difluorophenyl)acryloyl)phenyl)acrylamide (16)

Pale yellow powder, 58.2% yield, mp 203.9-205.1 °C. ^{1}H-NMR (600 MHz, DMSO-*d6*), δ: 10.535 (s, 1H, NH), 8.067 (d, *J*=8.4 Hz, 2H, Ar-H^{2}, Ar-H^{6}), 7.876 (t, *J*=15.3 Hz, 3H, Ar-H^{3}, Ar-H^{5}, β-H), 7.682 (d, *J*=16.2 Hz, 1H, α-H), 7.582-7.533 (m, 1H, Ar-H$^{4'}$), 7.258 (t, *J*=17.4 Hz, 2H, Ar-H$^{1'}$, Ar-H$^{5'}$), 6.498-6.453 (m, 1H, CO-CH), 6.321 (dd, *J*=1.8, 15.0 Hz, 1H, CH), 5.826 (dd, *J*=1.8, 8.4 Hz, 1H, CH). ^{13}C-NMR (400 MHz, DMSO), δ: 184.750, 164.376, 144.183, 132.985, 132.763, 132.709×2, 132.423, 130.195×2, 129.142, 128.933, 127.744, 119.842×2, 112.890×2, 112.732. HPLC: purity 95.8%. LC-MS m/z: 314.06[M+1]$^{+}$, calcd for $C_{18}H_{13}F_2NO_2$: 313.09 .

4.1.15 (E)-N-(4-(3-(3-fluorophenyl)acryloyl)phenyl)acrylamide (17)

Pale yellow powder, 61.4% yield, mp 143.3-145.1 °C. ^{1}H-NMR (600 MHz, DMSO-*d6*), δ: 10.540 (s, 1H, NH), 8.206 (d, *J*=9.0 Hz, 2H, Ar-H^{2}, Ar-H^{5}), 8.030 (d, *J*=15.6 Hz, 1H, β-H), 7.880 (s, 2H, Ar-H^{3}, Ar-H^{4}), 7.861 (d, *J*=5.4 Hz, 1H, α-H), 7.715 (t, *J*=8.4 Hz, 2H, Ar-H$^{6'}$, Ar-H$^{5'}$), 7.526-7.490 (m, 1H, Ar-H$^{4'}$), 7.294 (td, *J*=1.8, 6.0 Hz, 1H, Ar-H$^{2'}$), 6.509-6.464 (m, 1H, CO-CH), 6.333 (dd, *J*=1.8, 15.0 Hz, 1H, CH), 5.840 (dd, *J*=1.2, 8.4 Hz, 1H, CH). ^{13}C-NMR (400 MHz, DMSO), δ: 188.737, 163.616, 142.887, 142.266, 131.257, 130.491, 130.440, 129.949×2, 127.918, 124.310, 123.748, 119.654×2, 117.190, 117.051, 114.614, 114.464. HPLC: purity 95.1%. LC-MS m/z: 296.16[M+1]$^{+}$, calcd for $C_{18}H_{14}FNO_2$: 295.10.

4.1.16 N-(4-cinnamoylphenyl)acrylamide (18)

Pale yellow powder, 51.3% yield, mp 191.8-192.4 °C. ^{1}H-NMR (600 MHz, DMSO-*d6*), δ: 10.516 (s, 1H, NH), 8.178 (d, *J*=8.4 Hz, 2H, Ar-H^{2}, Ar-H^{6}), 7.949 (d, *J*=15.6 Hz, 1H, β-H), 7.893-7.855 (m, 4H, Ar-H^{3}, Ar-H^{5}, Ar-H$^{2'}$, Ar-H$^{6'}$), 7.729 (d, *J*=15.6 Hz, 1H, α-H), 7.461 (t, *J*=6.6 Hz, 3H, Ar-H$^{3'}$, Ar-H$^{4'}$, Ar-H$^{5'}$), 6.502-6.457 (m, 1H, CO-CH), 6.323 (dd, *J*=1.8, 15.0 Hz, 1H, CH), 5.828 (dd, *J*=1.8, 8.4 Hz, 1H, CH). ^{13}C-NMR (400 MHz, DMSO), δ: 188.995, 163.584, 144.629, 141.931, 134.979,

134.114, 130.831, 130.491, 129.969×2, 128.954×2, 128.685, 128.432×2, 121.865, 119.302. HPLC: purity 97.8%. LC-MS m/z: 278.06[M+1]$^+$, calcd for $C_{18}H_{15}NO_2$: 277.11.

4.1.17 (E)-N-(4-(3-(2,3-dimethoxyphenyl)acryloyl)phenyl)acrylamide (19)

Pale yellow powder, 62.4% yield, mp 166.1-167.7 °C. ^{1}H-NMR (600 MHz, DMSO-*d6*), δ: 10.517 (s, 1H, NH), 8.156 (d, *J*=9.0 Hz, 2H, Ar-H^2, Ar-H^6), 7.972 (d, *J*=7.8 Hz, 1H, β-H), 7.910-7.852 (m, 3H, Ar-H^3, Ar-H^5, α-H), 7.618 (t, *J*=9.0 Hz, 1H, Ar-H^5), 7.156 (d, *J*=4.8 Hz, 2H, Ar-H$^{4'}$, Ar-H$^{6'}$), 6.502-6.456 (m, 1H, CO-CH), 6.323 (d, *J*=17.4 Hz, 1H, CH), 5.828 (d, *J*=10.2 Hz, 1H, CH), 3.843 (s, 3H, OCH_3), 3.800 (s, 3H, OCH_3). ^{13}C-NMR (400 MHz, DMSO), δ: 189.352, 163.587, 153.268, 146.049, 141.888, 139.484, 134.216, 130.866, 129.995×2, 129.194, 128.608, 127.508, 124.171, 123.435, 119.751, 119.271, 114.318. HPLC: purity 98.3%. LC-MS m/z: 338.16[M+1]$^+$, calcd for $C_{20}H_{19}NO_4$: 337.13.

4.1.18 (E)-N-(4-(3-(2-(trifluoromethyl)phenyl)acryloyl)phenyl)acrylamide (20)

Pale yellow powder, 65.1% yield, mp 180.9-184.0 °C. ^{1}H-NMR (600 MHz, DMSO-*d6*), δ: 10.717 (s, 1H, NH), 8.280 (d, *J*=9.0 Hz, 1H, β-H), 8.200 (d, *J*=9.0 Hz, 2H, Ar-H^2, Ar-H^6), 8.059 (d, *J*=15.6 Hz, 1H, Ar-H^3) 7.959 (d, *J*=15.6 Hz, 1H, Ar-H^5), 7.907-7.886 (m, 3H, α-H, Ar-H$^{2'}$, Ar-H$^{6'}$), 7.817 (t, *J*=16.2 Hz, 1H, Ar-H$^{6'}$), 7.573 (d, *J*=6.6 Hz, 1H, Ar-H$^{4'}$), 6.526-6.490 (m, 1H, CO-CH), 6.328 (t, *J*=16.8 Hz, 1H, CH), 5.834 (d, *J*=10.2 Hz, 1H, CH). ^{13}C-NMR (400 MHz, DMSO), δ: 187.210, 163.639, 143.747, 137.240, 133.000, 132.894, 132.044, 130.330, 130.085×2, 128.717, 127.802, 126.260, 126.140, 126.094, 125.265, 118.812×2. HPLC: purity 97.7%. LC-MS m/z: 346.09[M+1]$^+$, calcd for $C_{19}H_{14}F_3NO_2$: 345.10.

4.1.19 (E)-N-(4-(3-(2,5-dimethoxyphenyl)acryloyl)phenyl)acrylamide (21)

Pale yellow powder, 60.32% yield, mp 173.3-176.5 °C. ^{1}H-NMR (600 MHz, DMSO-*d6*), δ: 10.527 (s, 1H, NH), 8.178 (d, *J*=9.0 Hz, 2H, Ar-H^2, Ar-H^6), 8.028 (d, *J*=15.6 Hz, 1H, β-H), 7.924 (d, *J*=15.6 Hz, 1H, α-H), 7.868 (d, *J*=8.4 Hz, 2H, Ar-H^3, Ar-H^5), 7.561 (d, *J*=2.4 Hz, 1H, Ar-H$^{4'}$), 7.050 (t, *J*=4.2 Hz, 2H, Ar-H$^{3'}$, Ar-H$^{6'}$), 6.508-6.463 (m, 1H, CO-CH), 6.330 (dd, *J*=1.8, 15.0 Hz, 1H, CH), 5.836 (dd, *J*=1.8, 16.8 Hz, 1H, CH), 3.852 (s, 3H, OCH_3), 3.811 (s, 3H, OCH_3). ^{13}C-NMR (400 MHz, DMSO), δ: 189.698, 163.841, 154.277, 153.773, 141.875, 139.936, 139.911, 131.358, 129.938 ×2, 127.711, 123.721, 119.551×2, 117.472, 114.435, 113.296, 56.482, 56.053. HPLC: purity 96.7%. LC-MS m/z: 338.16[M+1]$^+$, calcd for $C_{20}H_{19}NO_4$: 337.13.

4.1.20 (E)-N-(4-(3-(2-bromophenyl)acryloyl)phenyl)acrylamide (22)

Pale yellow powder, 67.56% yield, mp 191.8-192.4 °C. ^{1}H-NMR (600 MHz,

DMSO-*d6*), δ: 10.537 (s, 1H, NH), 8.190 (d, *J*=8.4 Hz, 3H, Ar-H^2, Ar-H^6, β-H), 7.974 (d, *J*=4.8 Hz, 2H, Ar-H^3, Ar-H^5), 7.870 (d, *J*=8.4 Hz, 2H, Ar-$H^{3'}$, α-H), 7.743 (d, *J*=7.8 Hz, 1H, Ar-$H^{6'}$), 7.496 (t, *J*=15.0 Hz, 1H, Ar-H^5), 7.401-7.376 (m, 1H, Ar-$H^{4'}$), 6.503-6.457 (m, 1H, CO-CH), 6.325 (dd, *J*=1.8, 15.0 Hz, 1H, CH), 5.831 (dd, *J*=1.2, 9.0 Hz, 1H, CH). ^{13}C-NMR (400 MHz, DMSO), δ: 187.346, 163.757, 163.630, 140.676, 134.107, 133.255, 132.232, 132.005, 131.526, 130.029×2, 128.704, 128.191, 127.814, 125.232, 124.965, 118.809×2. HPLC: purity 96.2%. LC-MS m/z: 355.93$[M+1]^+$, calcd for $C_{18}H_{14}BrNO_2$: 355.02.

4.1.21 (E)-N-(4-(3-(4-chlorophenyl)acryloyl)phenyl)acrylamide (23)

Pale yellow powder, 62.54% yield, mp 168.0-173.8 °C. ^{1}H-NMR (600 MHz, $CDCl_3$), δ: 8.057 (d, *J*=8.4 Hz, 2H, Ar-H^2, Ar-H^6), 7.790-7.765 (m, 3H, β-H, Ar-H^3, Ar-H^5), 7.560 (d, *J*=7.8 Hz, 2H, Ar-$H^{2'}$, Ar-$H^{6'}$), 7.534 (d, *J*=15.6 Hz, 1H, α-H), 7.417 (d, *J*=7.8 Hz, 2H, Ar-$H^{3'}$, Ar-$H^{5'}$), 6.515 (d, *J*=16.8 Hz, 1H, CO-CH), 6.349-6.304 (m, 1H, CH), 5.858 (d, *J*=10.2 Hz, 1H, CH). ^{13}C-NMR (400 MHz, DMSO), δ: 188.995, 163.584, 144.629, 141.931, 134.979, 134.114, 130.837, 130.491, 129.969×2, 128.954×2, 128.685, 128.432×2, 121.865, 119.302. HPLC: purity 98.9%. LC-MS m/z: 312.10$[M+1]^+$, calcd for $C_{18}H_{14}ClNO_2$: 311.07.

4.1.22 (E)-N-(4-(3-(3,4-dichlorophenyl)acryloyl)phenyl)acrylamide (24)

Pale yellow powder, 65.79% yield, mp 168.9-171.3 °C. ^{1}H-NMR (600 MHz, $CDCl_3$), δ: 8.057 (d, *J*=7.8 Hz, 2H, Ar-H^2, Ar-H^6), 7.966 (t, *J*=7.8 Hz, 1H, β-H), 7.786 (d, *J*=7.8 Hz, 2H, Ar-H^3, Ar-H^5), 7.735 (d, *J*=12.6 Hz, 3H, α-H, Ar-$H^{2'}$, Ar-$H^{3'}$), 7.284 (s, 1H, Ar-$H^{6'}$), 6.517 (d, *J*=16.8 Hz, 1H, CO-CH), 6.348-6.303 (m, 1H, CH), 5.864 (d, *J*=10.2 Hz, 1H, CH). ^{13}C-NMR (400 MHz, DMSO), δ: 187.239, 163.641, 143.742, 137.815, 135.059, 131.812, 131.506, 130.087×2, 129.830, 128.394, 127.840, 127.165, 123.211, 118.815×2, 118.725. HPLC: purity 95.4%. LC-MS m/z: 346.03$[M+1]^+$, calcd for $C_{18}H_{13}Cl_2NO_2$: 345.03.

4.1.23 (E)-N-(4-(3-(3,4-difluorophenyl)acryloyl)phenyl)acrylamide (25)

Pale yellow powder, 62.54% yield, mp 180.1-182.5 °C. ^{1}H-NMR (600 MHz, $CDCl_3$), δ: 8.057 (d, *J*=7.8 Hz, 2H, Ar-H^2, Ar-H^6), 7.966 (t, *J*=7.8 Hz, 1H, β-H), 7.786 (d, *J*=7.8 Hz, 2H, Ar-H^3, Ar-H^5), 7.735 (d, *J*=12.6 Hz, 4H, α-H, Ar-$H^{2'}$, Ar-$H^{2'}$, Ar-$H^{3'}$), 7.284 (s, 1H, Ar-$H^{6'}$), 6.517 (d, *J*=16.8 Hz, 1H, CO-CH), 6.348-6.303 (m, 1H, CH), 5.864 (d, *J*=10.2 Hz, 1H, CH). ^{13}C-NMR (400 MHz, DMSO), δ: 187.564, 164.095, 144.211, 137.143, 135.972, 135.565, 132.547×2, 131.900×2, 130.614, 130.322, 130.005, 128.437, 128.392, 125.780, 119.216×2. HPLC: purity 95.5%. LC-MS m/z: 314.02$[M+1]^+$, calcd for $C_{18}H_{13}F_2NO_2$: 313.09.

4.1.24 (E)-N-(4-(3-(3,4,5-trimethoxyphenyl)acryloyl)phenyl)acrylamide (26)

Pale yellow powder, 67.19% yield, mp 186.5-188.1 °C. ^{1}H-NMR (600 MHz, DMSO-*d6*), δ: 10.515 (s, 1H, NH), 8.188 (d, *J*=9.0 Hz, 2H, Ar-H^{2}, Ar-H^{6}), 7.910-7.865 (m, 3H, Ar-H^{3}, Ar-H^{5}, β-H), 7.683 (d, *J*=15.6 Hz, 1H, α-H), 7.229 (s, 2H, Ar-H$^{2'}$, Ar-H$^{6'}$), 6.502-6.456 (m, 1H, CO-CH), 6.323 (dd, *J*=1.8, 15.0Hz, 1H, CH), 5.829 (dd, *J*=1.2, 7.8 Hz, 1H, CH), 3.868 (s, 6H, OCH_3×2), 3.716 (s, 3H, OCH_3). ^{13}C-NMR (400 MHz, DMSO), δ: 189.050, 163.629, 153.543×2, 144.827×2, 141.922, 134.150, 130.842, 130.416, 129.931×2, 128.651, 121.243, 119.326×2, 105.588×2, 60.973, 56.297×2. HPLC: purity 96.9%. LC-MS m/z: 368.11[M+1]$^{+}$, calcd for $C_{21}H_{21}NO_5$: 367.14.

4.1.25 (E)-N-(4-(3-(3,4-dimethoxyphenyl)acryloyl)phenyl)acrylamide (27)

Pale yellow powder, 61.22% yield, mp 110.3-112.9 °C. ^{1}H-NMR (600 MHz, $CDCl_3$), δ: 8.059 (d, *J*=9.0 Hz, 2H, Ar-H^{2}, Ar-H^{6}), 7.782-7.755 (m, 3H, Ar-H^{3}, Ar-H^{5}, β-H), 7.421 (d, *J*=15.6 Hz, 1H, α-H), 7.261 (d, *J*=7.8 Hz, 1H, Ar-H$^{2'}$), 7.183 (d, *J*=1.2 Hz, 1H, Ar-H$^{5'}$), 6.926 (d, *J*=8.4 Hz, 1H, Ar-H$^{6'}$), 6.514 (d, *J*=16.8 Hz, 1H, CO-CH), 6.349-6.304 (m, 1H, CH), 5.853 (d, *J*=10.2 Hz, 1H, CH), 3.979 (s, 3H, OCH_3), 3.956 (s, 3H, OCH_3). ^{13}C-NMR (400 MHz, DMSO), δ: 189.681, 166.340, 151.531, 149.491, 148.728, 144.841×2, 143.228, 142.310, 129.869×2, 128.604, 127.827, 123.104, 111.294, 110.879, 110.394, 56.012×2. HPLC: purity 99.0%. LC-MS m/z: 338.16[M+1]$^{+}$, calcd for $C_{20}H_{19}NO_4$: 337.13.

4.1.26 (E)-N-(4-(3-(2,3-dichlorophenyl)acryloyl)phenyl)acrylamide (28)

Pale yellow powder, 67.88% yield, mp 205.3-208.1 °C. ^{1}H-NMR (600 MHz, DMSO-*d6*), δ: 10.565 (s, 1H, NH), 8.200 (dd, *J*=1.2, 8.4 Hz, 3H, β-H, Ar-H^{2}, Ar-H^{6}), 8.024 (d, *J*=3.6 Hz, 2H, Ar-H^{3}, Ar-H^{5}), 7.879 (d, *J*=9.0 Hz, 2H, α-H, Ar-H$^{3'}$), 7.749 (t, *J*=7.8 Hz, 1H, Ar-H$^{5'}$), 7.490 (t, *J*=15.6 Hz, 1H, Ar-H$^{6'}$), 6.510-6.465 (m, 1H, CO-CH), 6.332 (dd, *J*=1.8, 8.4 Hz, 1H, CH), 5.841 (dd, *J*=1.8, 8.4 Hz, 1H, CH). ^{13}C-NMR (400 MHz, DMSO), δ: 187.239, 163.641, 143.742, 137.815, 135.059, 131.812, 131.506, 130.087×2, 129.830, 128.394, 127.821, 127.165, 126.211, 118.815×2, 118.725. HPLC: purity 98.6%. LC-MS m/z: 346.03[M+1]$^{+}$, calcd for $C_{18}H_{13}Cl_2NO_2$: 345.03.

4.1.27 (E)-N-(4-(3-(2-fluoro-5-methoxyphenyl)acryloyl)phenyl)acrylamide (29)

Pale yellow powder, 67.88% yield, mp 151.2-154.7 °C. ^{1}H-NMR (600 MHz, $CDCl_3$), δ: 8.054 (d, *J*=8.4 Hz, 2H, Ar-H^{2}, Ar-H^{6}), 7.884 (s, 1H, β-H), 7.785 (d, *J*=8.4 Hz, 2H, Ar-H^{3}, Ar-H^{5}), 7.634 (d, *J*=16.2 Hz, 1H, α-H), 7.121 (s, 1H, Ar-H$^{3'}$), 7.070 (t, *J*=18.6 Hz, 1H, Ar-H$^{4'}$), 6.939-6.919 (m, 1H, Ar-H$^{6'}$), 6.510 (d, *J*=16.8 Hz, 1H, CO-CH), 6.361-6.216 (m, 1H, CH), 5.848 (d, *J*=10.2 Hz, 1H, CH), 3.852 (s, 3H,

OCH_3). ^{13}C-NMR (400 MHz, DMSO), δ: 188.997, 163.683, 155.856, 142.152, 137.367, 133.831, 130.381×2, 130.852, 130.041, 124.609, 124.553, 119.345, 117.403, 117.336, 116.969, 116.776, 113.673, 55.896. HPLC: purity 95.6%. LC-MS m/z: 326.19$[M+1]^+$, calcd for $C_{19}H_{16}FNO_3$: 325.11.

4.2 Synthetic procedures

4.2.1 General procedure for synthesis of chalcone derivatives **2-9** and **11**

A mixture of compound **1** or **10** (1 mmol), various acyl chloride (2 mmol), and anhydrous THF (10 mL) at 0 °C condition with triethylamine as a catalyst and stirred for 30 min. Then the resulting mixture was then allowed slowly to warm to room temperature. When TLC monitoring showed complete consumption of the starting material, the reaction mixture was evaporated under reduced pressure. Then, the mixture was extracted with CH_2Cl_2 and water. Subsequently, the resulting mixture was washed with brine, dried by Na_2SO_4, and concentrated in vacuo to provide residue. Finally, the residue was purified by silica gel column to obtain desired products.

4.2.2 General procedure for synthesis of chalcone derivatives **12-29**

A mixture of compound **11** (1 mmol), a variety of substituted benzaldehyde, and 40% NaOH in EtOH (10 mL), stirred at room temperature for 12 h. Then, the reaction mixture concentrated in vacuo to provide residue. Finally, the residue was purified by silica gel column to obtain desired products.

4.3 Cells culture

The human lung cancer cell line NCI-H460 was obtained directly from the Institute of Biochemistry and Cell Biology, Chinese Academy of Sciences. Human lung cancer cell line A549 was purchased from the Cell Bank of the Chinese Academy of Sciences (Wuhan, China). And human lung cancer cell line H1975 was purchased from the Shanghai Institute of Biosciences and Cell Resources Center (Shanghai, China). Three cell lines were grown in RPMI-1640 medium (Gibco) supplemented with 10% fetal bovine serum (FBS, Gibco), 100 U/mL penicillin and 100 mg/mL streptomycin (Gibco). All cell lines were cultured at 37 °C in a humidified atmosphere containing 5% CO_2. Furthermore, cells were used for the appropriate experiments until growing to the logarithmic phase. BMS-345541, xanthohumol, dimethyl sulfoxide (DMSO) and MTT were purchased from Sigma-Aldrich (St. Louis, MO).

4.4 MTT assay

Lung cancer cell lines NCI-H460, A549 and H1975 were seeded in 96-well plate with 3000 per well, and exposed to compounds for indicated times after overnight

culturing. Then 20 μL solution of 3-(4,5-dimethylthiazol-2-yl)-2,5-diphenyltetrazolium bromide (MTT) (5 mg/mL) was added to every well. After 4 h incubation, 150 μL of DMSO was added to dissolve the formazan crystals of intracellular and the absorbance (A value) was measured at 490 nm using an Enzyme-labeled meter (MD, USA). Therefore, the percentage of inhibitory effect was calculated as [1－value of compound-treated group (A)/control group (A)]×100%, and the values of IC_{50} were determined through Prism 5 (GraphPad Software).

4.5 Colony formation assay

The colony formation assay was performed to evaluate the effect of analogs on proliferation. NCI-H460 cells were seeded in 6-well plate with 1000 per well and incubated with compounds for 12 h after overnight growth. Next, medium was changed and cells were cultured for approximately 8 days with normal medium. At last, cells were combined with crystal violet and images were obtained with camera.

4.6 Intracellular ROS determined by flow cytometry

Influences of compound **8** on ROS generation were assessed by flow cytometry. NCI-H460 cells were cultured in 6-well plate for 24 h with 300, 000/well and then treated with compounds for a certain time in the absence or presence of NAC. Then medium was changed to serum-free medium and cells were incubated with DCFH-DA (10 μM) (Beyotime Institute of Biotechnology, China) for 30 min at 37 °C in the dark. Finally, the cells were collected and the samples were analyzed by flow cytometry (BD, USA).

4.7 Western blot analysis

NCI-H460 cells were growing in the 6-well plate for 24 h and then exposed to compound **8** for indicated times. Next, cells were lysed with lysis solution on the ice. The concentrations of protein were detected by the Bradford colorimetric method. After that, samples were separated through sodium dodecyl sulfate-polyacrylamide gel electrophoresis (SDS-PAGE) (10% acrylamide gels) and transferred to PVDF. 5% skim milk was used to block the PVDF membranes before staining with the primary antibodies against caspase-3 and β-actin (Cell Signaling Technology, USA) at 4 °C. After overnight, membranes were incubated with secondary antibody for 1 h at room temperature and the immune-reactive complexes were tested with ECL (Enhanced chemiluminescence kit) (Bio-Rad, Hercules, CA). Determination analysis was performed using the Image Lab Software 5.1 (Bio-Rad).

4.8 Determination of pyroptosis in NCI-H460 cells

To detect the morphology of pyroptosis cells, NCI-H460 cell lines were seeded

into 6-well plate with 300, 000/well 24 h before stimulation. Cells were exposed to 20 μg/mL cisplatin (24 h) and 20 μM compound **8** (19 and 24 h) in the presence or absence of NAC (20 mmol/L). Static bright field cell images were obtained with microscopic imaging (Nikon, Japan). Cells subjected to DMSO were used as control group.

4.9 *In vivo* toxicity examination

Wild-type BALB/c mice (male) were purchased from Shanghai Slaccas Lab Animal Co. Ltd. The 18 mice (26-33 g) were randomly divided into 3 groups (n=6), including vehicle group, EF24 group and compound **8** group. Toxicity examination was performed with compounds (500 mg/Kg) via intraperitoneal (ip) injection at the first day only. All the mice were housed under 12 h light-dark cycles at 25 °C and free for water and diet. In addition, the mortality of the animals within 14 days was kept a record. Then these mice were euthanasia together.

4.10 Statistical analysis

These data were presented as mean±standard error (SEM) for three independent experiments. Statistical comparisons among results were performed using one-way analysis of variance (ANOVA). $P<0.05$ was set as the criterion of statistical significance.

Acknowledgment

The work was supported by Zhejiang Province Natural Science Funding of China (LY15H280014, LY17H160059, LQ18H280008), the Technology Foundation for Medical Science of Zhejiang Province (2015KYA1506), the National Natural Science Foundation of China (81803580, 81272462), Project of Wenzhou Sci-Tech Bureau (Y20170158) and Granted by the Opening Project of Zhejiang Provincial Top Key Discipline of Pharmaceutical Sciences.

References

[1] A. Vachani, L.V. Sequist, A. Spira, AJRCCM: 100-year anniversary. The shifting landscape for lung cancer: Past, present, and future, American Journal of Respiratory and Critical Care Medicine, 195 (2017) 1150-1160.

[2] W.-L. Tan, A. Jain, A. Takano, E.W. Newell, N.G. Iyer, W.-T. Lim, E.-H. Tan, W. Zhai, A.M. Hillmer, W.-L. Tam, D.S.W. Tan, Novel therapeutic targets on the horizon for lung cancer, The Lancet Oncology, 17 (2016) e347-e362.

[3] F.R. Hirsch, G.V. Scagliotti, J.L. Mulshine, R. Kwon, W.J. Curran, Y.-L. Wu, L. Paz-Ares, Lung cancer: Current therapies and new targeted treatments, The Lancet, 389 (2017) 299-311.

[4] C. Coppola, A. Rienzo, G. Piscopo, A. Barbieri, C. Arra, N. Maurea, Management of QT prolongation induced by anti-cancer drugs: Target therapy and old agents. Different algorithms for different drugs, Cancer Treatment Reviews, 63 (2018) 135-143.

[5] P. Qiu, S. Zhang, Y. Zhou, M. Zhu, Y. Kang, D. Chen, J. Wang, P. Zhou, W. Li, Q. Xu, R. Jin, J. Wu, G. Liang, Synthesis and evaluation of asymmetric curcuminoid analogs as potential anticancer agents that downregulate NF-κB activation and enhance the sensitivity of gastric cancer cell lines to irinotecan chemotherapy, European Journal of Medicinal Chemistry, 139 (2017) 917-925.

[6] S. Wang, K. Fang, G. Dong, S. Chen, N. Liu, Z. Miao, J. Yao, J. Li, W. Zhang, C. Sheng, Scaffold diversity inspired by the natural product evodiamine: Discovery of highly potent and multitargeting antitumor agents, Journal of Medicinal Chemistry, 58 (2015) 6678-6696.

[7] G. Kallifatidis, J.J. Hoy, B.L. Lokeshwar, Bioactive natural products for chemoprevention and treatment of castration-resistant prostate cancer, Seminars in Cancer Biology, 40-41 (2016) 160-169.

[8] C. Zhuang, W. Zhang, C. Sheng, W. Zhang, C. Xing, Z. Miao, Chalcone: A privileged structure in medicinal chemistry, Chemical Reviews, 117 (2017) 7762-7810.

[9] V.R. Yadav, S. Prasad, B. Sung, B.B. Aggarwal, The role of chalcones in suppression of NF-kappaB-mediated inflammation and cancer, International Immunopharmacology, 11 (2011) 295-309.

[10] M.N. Gomes, E.N. Muratov, M. Pereira, J.C. Peixoto, L.P. Rosseto, P.V.L. Cravo, C.H. Andrade, B.J. Neves, Chalcone derivatives: Promising starting points for drug design, Molecules, 22 (2017) 1210-1234.

[11] J. Wu, C. Wang, Y. Cai, J. Peng, D. Liang, Y. Zhao, S. Yang, X. Li, X. Wu, G. Liang, Synthesis and crystal structure of chalcones as well as on cytotoxicity and antibacterial properties, Medicinal Chemistry Research, 21 (2011) 444-452.

[12] J. Wu, J. Li, Y. Cai, Y. Pan, F. Ye, Y. Zhang, Y. Zhao, S. Yang, X. Li, G. Liang, Evaluation and discovery of novel synthetic chalcone derivatives as anti-inflammatory agents, Journal of Medicinal Chemistry, 54 (2011) 8110-8123.

[13] J. Wu, C. Cheng, L. Shen, Z. Wang, S. Wu, W. Li, S. Chen, R. Zhou, P. Qiu, Synthetic chalcones with potent antioxidant ability on H_2O_2-induced apoptosis in PC12 cells, International Journal of Molecular Sciences, 15 (2014) 18525-18539.

[14] B. Srinivasan, T.E. Johnson, R. Lad, C. Xing, Structure-activity relationship studies of chalcone leading to 3-hydroxy-4,3',4',5'-tetramethoxychalcone and its analogues as potent nuclear factor kappaB inhibitors and their anticancer activities, Journal of Medicinal Chemistry, 52 (2009) 7228-7235.

[15] C.W. Mai, M. Yaeghoobi, N. Abd-Rahman, Y.B. Kang, M.R. Pichika, Chalcones with electron-withdrawing and electron-donating substituents: Anticancer activity against TRAIL resistant cancer cells, structure–activity relationship analysis and regulation of apoptotic proteins, European Journal of Medicinal Chemistry, 77 (2014) 378-387.

[16] N. Shankaraiah, S. Nekkanti, U.R. Brahma, N. Praveen Kumar, N. Deshpande, D. Prasanna, K.R. Senwar, U. Jaya Lakshmi, Synthesis of different heterocycles-linked chalcone conjugates as cytotoxic agents and tubulin polymerization inhibitors, Bioorganic & Medicinal Chemistry, 25 (2017) 4805-4816.

[17] S. Rana, E.C. Blowers, C. Tebbe, J.I. Contreras, P. Radhakrishnan, S. Kizhake, T. Zhou, R.N.

Rajule, J.L. Arnst, A.R. Munkarah, R. Rattan, A. Natarajan, Isatin derived spirocyclic analogues with alpha-methylene-gamma-butyrolactone as anticancer agents: A structure-activity relationship study, Journal of Medicinal Chemistry, 59 (2016) 5121-5127.

[18] L. Heller, S. Schwarz, V. Perl, A. Kowitsch, B. Siewert, R. Csuk, Incorporation of a Michael acceptor enhances the antitumor activity of triterpenoic acids, European Journal of Medicinal Chemistry, 101 (2015) 391-399.

[19] P.A. Jackson, J.C. Widen, D.A. Harki, K.M. Brummond, Covalent modifiers: A chemical perspective on the reactivity of alpha,beta-unsaturated carbonyls with thiols via hetero-Michael addition reactions, Journal of Medicinal Chemistry, 60 (2017) 839-885.

[20] Y. Li, L. Zhang, F. Dai, W. Yan, H. Wang, Z. Tu, B. Zhou, Hexamethoxylated mono-carbonyl analogues of curcumin cause G2/M cell cycle arrest in NCI-H460 cells via Michael acceptor-dependent redox intervention, Journal of Agricultural and Food Chemistry, 63 (2015) 7731-7742.

[21] S.M. Raja, R.J. Clubb, C. Ortega-Cava, S.H. Williams, T.A. Bailey, L. Duan, X. Zhao, A.L. Reddi, A.M. Nyong, A. Natarajan, V. Band, H. Band, Anticancer activity of Celastrol in combination with ErbB2-targeted therapeutics for treatment of ErbB2-overexpressing breast cancers, Cancer Biology & Therapy, 11 (2014) 263-276.

[22] M. Gersch, J. Kreuzer, S.A. Sieber, Electrophilic natural products and their biological targets, Natural Product Reports, 29 (2012) 659-682.

[23] L. Wang, H. Li, M. Li, S. Wang, X. Jiang, Y. Li, G. Ping, Q. Cao, X. Liu, W. Fang, G. Chen, J. Yang, C. Wu, SL4, a chalcone-based compound, induces apoptosis in human cancer cells by activation of the ROS/MAPK signalling pathway, Cell Proliferation, 48 (2015) 718-728.

[24] W. Wu, H. Ye, L. Wan, X. Han, G. Wang, J. Hu, M. Tang, X. Duan, Y. Fan, S. He, L. Huang, H. Pei, X. Wang, X. Li, C. Xie, R. Zhang, Z. Yuan, Y. Mao, Y. Wei, L. Chen, Millepachine, a novel chalcone, induces G2/M arrest by inhibiting CDK1 activity and causing apoptosis via ROS-mitochondrial apoptotic pathway in human hepatocarcinoma cells *in vitro* and *in vivo*, Carcinogenesis, 34 (2013) 1636-1643.

[25] B. Zhang, D. Duan, C. Ge, J. Yao, Y. Liu, X. Li, J. Fang, Synthesis of xanthohumol analogues and discovery of potent thioredoxin reductase inhibitor as potential anticancer agent, Journal of Medicinal Chemistry, 58 (2015) 1795-1805.

[26] C.T. Chang, Y.C. Hseu, V. Thiyagarajan, K.Y. Lin, T.D. Way, M. Korivi, J.W. Liao, H.L. Yang, Chalcone flavokawain B induces autophagic-cell death via reactive oxygen species-mediated signaling pathways in human gastric carcinoma and suppresses tumor growth in nude mice, Archives of Toxicology, 91 (2017) 3341-3364.

[27] D.K. Mahapatra, S.K. Bharti, V. Asati, Anti-cancer chalcones: Structural and molecular target perspectives, European Journal of Medicinal Chemistry, 98 (2015) 69-114.

[28] Y. Nadatani, X. Huo, X. Zhang, C. Yu, E. Cheng, Q. Zhang, K.B. Dunbar, A. Theiss, T.H. Pham, D.H. Wang, T. Watanabe, Y. Fujiwara, T. Arakawa, S.J. Spechler, R.F. Souza, NOD-like receptor protein 3 inflammasome priming and activation in barrett's epithelial cells, Cellular and Molecular Gastroenterology and Hepatology, 2 (2016) 439-453.

[29] G.Y. Chen, G. Nunez, Inflammasomes in intestinal inflammation and cancer, Gastroenterology, 141 (2011) 1986-1999.

[30] C. Lin, J. Zhang, Inflammasomes in inflammation-induced cancer, Frontiers in Immunology, 8 (2017) 271-292.

[31] Y. Wang, W. Gao, X. Shi, J. Ding, W. Liu, H. He, K. Wang, F. Shao, Chemotherapy drugs induce pyroptosis through caspase-3 cleavage of a gasdermin, Nature, 547 (2017) 99-103.

[32] Y. Wang, B. Yin, D. Li, G. Wang, X. Han, X. Sun, GSDME mediates caspase-3-dependent pyroptosis in gastric cancer, Biochemical and Biophysical Research Communications, 495 (2018) 1418-1425.

[33] V. Derangere, A. Chevriaux, F. Courtaut, M. Bruchard, H. Berger, F. Chalmin, S.Z. Causse, E. Limagne, F. Vegran, S. Ladoire, B. Simon, W. Boireau, A. Hichami, L. Apetoh, G. Mignot, F. Ghiringhelli, C. Rebe, Liver X receptor beta activation induces pyroptosis of human and murine colon cancer cells, Cell Death and Differentiation, 21 (2014) 1914-1924.

[34] E. Gilberg, S. Jasial, D. Stumpfe, D. Dimova, J. Bajorath, Highly promiscuous small molecules from biological screening assays include many pan-assay interference compounds but also candidates for polypharmacology, Journal of Medicinal Chemistry, 59 (2016) 10285-10290.

[35] S.J. Capuzzi, E.N. Muratov, A. Tropsha, Phantom PAINS: Problems with the utility of alerts for pan-assay interference compounds, Journal of Chemical Information and Modeling, 57 (2017) 417-427.

[36] D. Lagorce, N. Oliveira, M.A. Miteva, B.O. Villoutreix, Pan-assay interference compounds (PAINS) that may not be too painful for chemical biology projects, Drug Discovery Today, 22 (2017) 1131-1133.

[37] A. Costa, A. Scholer-Dahirel, F. Mechta-Grigoriou, The role of reactive oxygen species and metabolism on cancer cells and their microenvironment, Seminars in Cancer Biology, 25 (2014) 23-32.

[38] L. Chen, Q. Li, B. Weng, J. Wang, Y. Zhou, D. Cheng, T. Sirirak, P. Qiu, J. Wu, Design, synthesis, anti-lung cancer activity, and chemosensitization of tumor-selective MCACs based on ROS-mediated JNK pathway activation and NF-κB pathway inhibition, European Journal of Medicinal Chemistry, 151 (2018) 508-519.

[39] X. Liu, K. Rothe, R. Yen, C. Fruhstorfer, T. Maetzig, M. Chen, D.L. Forrest, R.K. Humphries, X. Jiang, A novel AHI-1-BCR-ABL-DNM2 complex regulates leukemic properties of primitive CML cells through enhanced cellular endocytosis and ROS-mediated autophagy, Leukemia, 31 (2017) 2376-2387.

[40] J. Wu, S. Wu, L. Shi, S. Zhang, J. Ren, S. Yao, D. Yun, L. Huang, J. Wang, W. Li, X. Wu, P. Qiu, G. Liang, Design, synthesis, and evaluation of asymmetric EF24 analogues as potential anti-cancer agents for lung cancer, European Journal of Medicinal Chemistry, 125 (2017) 1321-1331.

[41] P. Poprac, K. Jomova, M. Simunkova, V. Kollar, C.J. Rhodes, M. Valko, Targeting free radicals in oxidative stress-related human diseases, Trends in Pharmacological Sciences, 38 (2017) 592-607.

[42] Y. Ai, B. Zhu, C. Ren, F. Kang, J. Li, Z. Huang, Y. Lai, S. Peng, K. Ding, J. Tian, Y. Zhang, Discovery of new monocarbonyl ligustrazine-curcumin hybrids for intervention of drug-sensitive and drug-resistant lung cancer, Journal of Medicinal Chemistry, 59 (2016) 1747-1760.

[43] L. Raj, T. Ide, A.U. Gurkar, M. Foley, M. Schenone, X. Li, N.J. Tolliday, T.R. Golub, S.A. Carr, A.F. Shamji, A.M. Stern, A. Mandinova, S.L. Schreiber, S.W. Lee, Selective killing of cancer cells by a small molecule targeting the stress response to ROS, Nature, 475 (2011)

231-234.

[44] A. Sun, Y.J. Lu, H. Hu, M. Shoji, D.C. Liotta, J.P. Snyder, Curcumin analog cytotoxicity against breast cancer cells: Exploitation of a redox-dependent mechanism, Bioorganic & Medicinal Chemistry Letters, 19 (2009) 6627-6631.

[45] B.K. Adams, J. Cai, J. Armstrong, M. Herold, Y. Lu, A. Sun, J.P. Snyder, D.C. Liotta, D.P. Jones, M. Shoji, EF24, a novel synthetic curcumin analog, induces apoptosis in cancer cells via a redox-dependent mechanism, Anti-Cancer Drugs, 16 (2005) 263-275.

[46] D. Subramaniam, R. May, S.M. Sureban, K.B. Lee, R. George, P. Kuppusamy, R.P. Ramanujam, K. Hideg, B.K. Dieckgraefe, C.W. Houchen, S. Anant, Diphenyl difluoroketone: A curcumin derivative with potent *in vivo* anticancer activity, Cancer Research, 68 (2008) 1962-1969.

[47] R. Jin, Q. Chen, S. Yao, E. Bai, W. Fu, L. Wang, J. Wang, X. Du, T. Wei, H. Xu, C. Jiang, P. Qiu, J. Wu, W. Li, G. Liang, Synthesis and anti-tumor activity of EF24 analogues as IKKbeta inhibitors, European Journal of Medicinal Chemistry, 144 (2017) 218-228.

Highlights

1. Incorporation of a α,β-unsaturated ketone functionality into chalcone can significantly improve the cytotoxicity.
2. Compound **8** showed more excellent inhibitory activity than positive controls against several kinds of lung cancer cells.
3. Compound **8** was able to trigger ROS-mediated pyroptosis in NCI-H460 cells.